URSI GASS 2020, Rome, Italy, 29 August - 5 September 2020

DTV radio spectrum anomaly detection based on an improved GAN

Liu Zhang(1), Chong Xing Huang (2), Hao Tang(3), Jing Jing Yang* (1), and Ming Huang* (1)
(1)School of Information Science and Engineering, Wireless Innovation Lab. of Yunnan University, Kunming 650091, China
(2) School of Management, Tianjin University of Commerce, TianJin, 300134, China
(3)Yunnan Radio Monitoring Station of the State Radio monitoring center, Kunming 650031, China
* yangjingjing@ynu.edu.cn; huangming@ynu.edu.cn

Abstract

Detecting anomalous behavior in radio spectrum is an urgent task due to the popularity of wireless applications. Radio spectrum anomalies include both the anomalies in authorized and unauthorized frequency band. In this paper, we focus on unsupervised radio spectrum Anomaly detection of Digital Television (DTV) frequency band (474MHz). Firstly, an improved GAN model was proposed and its efficacy was demonstrated on a MNIST dataset. Then, the model is trained by collecting the spectrum data sets at DTV band. The performance of the model was tested by simulating different interference signals. Results show that when the width and power of the interference pulse is 1.5MHz and 5dB greater than the signal, the detection accuracy achieves 97.86%. Besides, for a real FM interference signal with power of -15dBm, the detection rate is nearly 90%.

1 Introduction

Spectrum anomaly detection is the essential task for radio spectrum management. Energy detection is widely used in traditional radio monitoring system [1]. However, this method is ineffective for detecting the anomalies in authorized spectrum in use. Therefore, some statistical and machine learning methods have been proposed. For example, the bayesian approach for spectrum sensing, denoising and anomaly detection [2], spectrum anomalies detection using hidden markov models [3], and recurrent neural for radio anomaly detection [4]. The problem of learning the probability distribution of data is one of the most fundamental problems in statistics and machine learning. Due to Generative Adversarial Networks (GANs) provides optimal solutions for learning data true distributions, it becomes a hot spot in anomaly detection [5-7].

Recently, some unsupervised anomaly detection methods such as ANOGAN [8], GANomaly[9] have been proposed. These models were trained only on normal data without the need of abnormal data. Inspired by GANomaly, we propose an improved GAN model for radio spectrum anomaly detection, and the improved model is training faster and more stable. The rest of the paper is arranged as follows. Firstly, the efficacy of the improved model is demonstrated on a benchmark dataset [10]. Secondly, real-time spectrum of digital television are collected for training the model, and pulse-like interferences with a range of powers and width are added for abnormal detection test. Finally, real interferences occurring at the DTV frequency band are collected for testing the model.

2 Methodology & dataset

There is an encoder-decoder-encoder sub-networks in the generator of GANomaly, which may cause unstable training. For stable training, we made some improvements to GANnomaly model. First, we removed the second encoder behind Generator. It is well known that original GAN is not stable and hard to train, so we replace WGAN with GAN to train the improved model, the process of model training is more stable and faster after improvements.

The improved GAN model for radio anomaly detection is shown in Figure 1. We map radio spectrum images to latent space by convolutional neural networks (CNN) as the encoder, then generator as the decoder learn to reconstruct spectrum images from latent space by minimizing the distance between input images and reconstructed images. The discriminator will help training the generator.

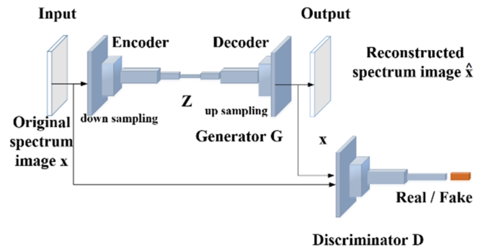

Figure 1. Structure of improved GAN model

Performance of the improved GAN model is demonstrated on MNIST dataset and compared with ANOGAN and GANomaly. Figure 2 shows that the improved model is training faster than ANOGAN and GANomaly, and obviously, the quality of improved generative models is better.

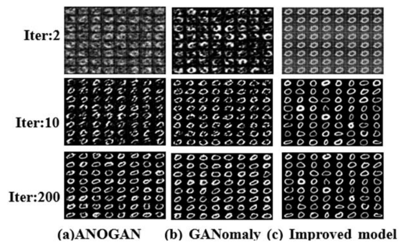

Figure 2. The performance of reconstruction on above three models

The improved model is mainly comprised by generator and discriminator as shown in Figure 1. The generator is a decoder-alike network that learns the distribution of input spectrum data from a latent space. Encoder network squeezes the input radio spectrum images to a latent space with 200 dimensions, extract important features [11] of input images, and help generator training. We used the Earth Mover (EM) distance to train our model.

Let $\mathbf{P}_r$ be a fixed distribution of input dataset χ , $\mathbf{P}_g$ be the distribution of reconstructed data by generator, so EM distance is

$$W\left(\mathbf{P}_r,\mathbf{P}_g\right)=\inf_{\gamma\in\Pi\left(\mathbf{P}_r,\mathbf{P}_g\right)}\mathbf{E}_{(x,y)\sim\gamma}\left[\|x-y\|\right], \qquad (1)$$

where $\Pi\left(\mathbf{P}_r,\mathbf{P}_g\right)$ denotes the set of all joint distribution $\gamma(x,y)$ whose marginal are respectively $\mathbf{P}_r$ and $\mathbf{P}_g$. Intuitively, $\gamma(x,y)$ indicates how much "mass" must be transported from x to y in order to transform the distributions $\mathbf{P}_r$ into the distribution $\mathbf{P}_g$. The EM distance then is the "cost" of the optimal transport plan. When training WGAN, Arjovsky et al. [12] gave a roughly approximate to EM distance, by using Weight clipping in WGAN model, minimizing the EM distance between input images and reconstructed images, to make $\mathbf{P}_r$ as close as possible to $\mathbf{P}_g$.

During anomaly detection, we train the model only on normal radio spectrum images. Once model training finished, we assume that the generator has learned the distribution of input normal images so that when abnormal images is forward-passed into the model, the generator will not be able to reconstruct the abnormalities. Then we compute the residual of input images and reconstructed as follows:

$$r_i = \frac{\sum \left|\hat{x}_i - x_i\right|}{m \times n}, \qquad (2)$$

where $m\times n$ denotes size of input radio spectrum images, $\hat{x}_i$ is the *ith* reconstructed image by generator, x_i is the *ith* input image, r_i is corresponding residual.

$$output_i=\begin{cases}\text{normal}, r_i\le \text{threshold}\\ \text{abnormal}, r_i\ge \text{threshold}\end{cases} \qquad (3)$$

When r_i is over the threshold, the input spectrum image will be judged to an abnormal spectrum data.

Our experiments are carried out on the dataset collected using the receiver for 24 hours. The frequency range is from 467 MHz to 479 MHz, while the resolution bandwidth is 0.015 MHz. In order to evaluate the detection performance, we add pulse interference to the original spectrum as the abnormal data. the width of the pulse varies from 0.15 MHz to 1.5 MHz, powers range from 3db to 20db. The above abnormal data are sampled 1000 samples each. The spectra are collected with the equipment shown in Figure 3. Spectrum images with size

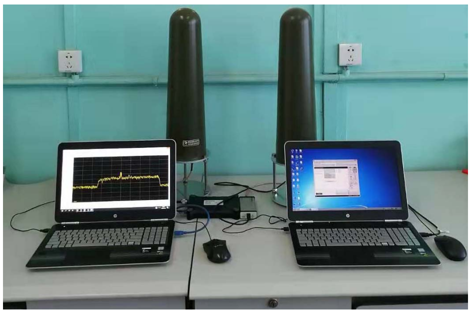

Figure 3. Receiver (left) and transmitter (right)

of 168×224 are sampled. Model uses convolutional architecture with stride 2, trained with RMSprop using a learning rate of 0.0002 and a batch size of 32.

3 Results

The normal radio spectrum data (images) are split into two data sets, one for training, and another for testing. The proposed model is trained on normal spectrum data, and tested on abnormal spectrum data. We compared the performance of the proposed GAN model for the detection of pulse interferences with different width and power. The experimental results are given in Figure 4

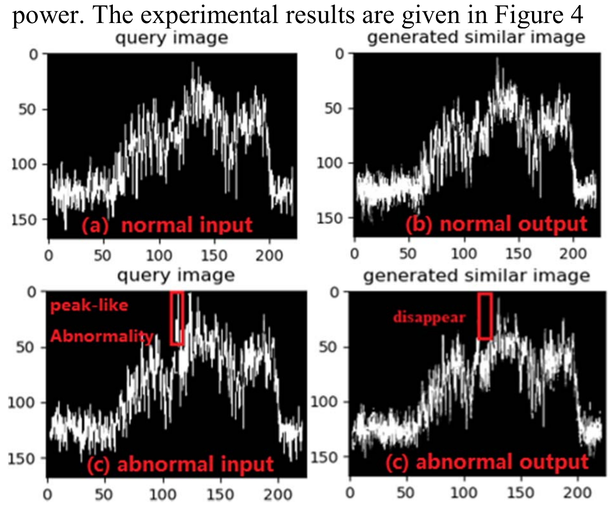

Figure 4. Process of detection for both normal and abnormal spectrum images

From panels (a) and (b), it is seen that when normal spectrum is put into the trained model, it can reconstruct the same image with normal input, while abnormal spectrum image is feed into, the model reconstructs the image the same as the normal image since we trained the model only with normal spectrum data. As a consequence, the abnormal spectrum can be detected through computing the residual.

We found that the accuracy of anomaly detection is closely related to the width and power of the added pulse interference. When both the width and power of pulse interferences are small, the model can hardly detect the abnormal radio spectrum, and the detection accuracy is about 54%. When we increase the bandwidth and power of pulse, the accuracy increases to 97.86%. Figure 5 demonstrates a clear separation within the residual when we increase the bandwidth of pulse interference. The results are listed in table 1.

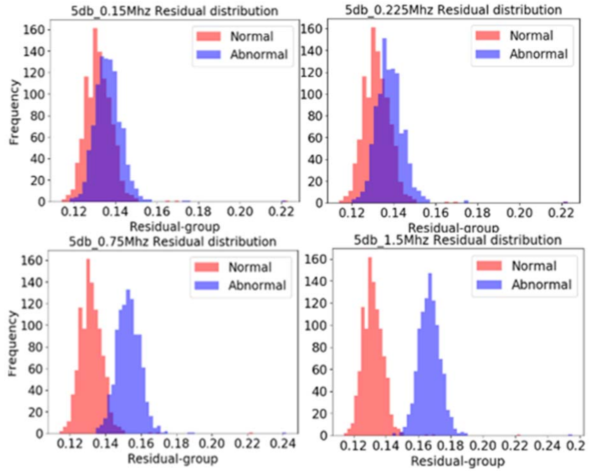

Figure 5. Histogram of the residuals for both normal and abnormal spectrum data

TABLE 1. Accuracy Rate of anomaly detection for different abnormalities

band / power	0.15Mhz	0.225Mhz	0.75Mhz	1.5Mhz
3db	53.75%	56.20%	74.70%	88.20%
5db	62.90%	69.70%	86.50%	93.93%
10db	71.40%	78.90%	91.20%	95.26%
15db	82.10%	90.25%	93.10%	96.52%
20db	89.35%	92.50%	95.30%	97.86%

Figure 6 and Figure 7 show the simulated ROC curve and anomaly detection accuracy. It is seen that the model gets better performance for anomaly detection when the pulse interference has a higher power and wider width. Besides, to explore the potential application of the improve GAN model, we transmit a FM signal with power of -35dbm, -25dbm and -15dbm, and collect the spectrum data in the DTV frequency band (474MHz) using the setup shown in Fig. 3. Results show that the detection rate is nearly 90% when transmitting power is -15dBm.

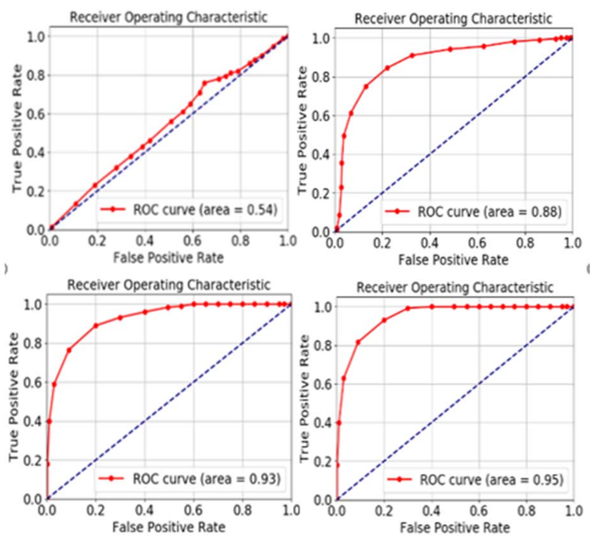

Figure 4. The ROC curve of detection results.

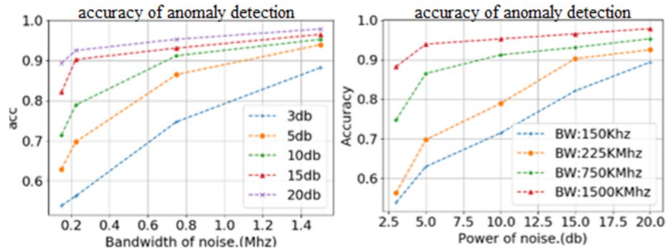

Figure 5. Accuracy of anomaly detection for the pulse interference with different power and width.

4 Conclusions

We proposed an improved GAN model for DTV radio spectrum anomaly detection. The dependence of detection accuracy on interference power and width is studied. The detection accuracy achieves 97.86% for a simulated interference pulse with power of 5dB and width of 1.5MHz. Besides, to explore the potential application of the improve GAN model, the DTV radio spectrum with FM interference signal is collected for the testing. Results show that the detection rate is nearly 90% when transmitting power is –15dBm. A commercial prototype for DTV radio spectrum anomaly detection is under development and more details will be published latter.

5 Acknowledgements

Our work was funded by the National Natural Science Foundation of China (Grant Nos. 61863035, 61963037, 11564044).

6 References

[1] D. Chen, J. Yang, J. Wu, H. Tang and M. Huang, "Spectrum occupancy analysis based on radio monitoring network," 2012 1st IEEE International Conference on Communications in China (ICCC), Beijing, China, August 15-17, 2012.

[2] E. Axell and E. G. Larsson, "A Bayesian approach to spectrum sensing, denoising and anomaly detection," 2009 IEEE International Conference on Acoustics, Speech and Signal Processing, Taipei, Taiwan, April 19-24, 2009.

[3] W. Honghao, J. Yunfeng and W. Lei, "Spectrum anomalies autonomous detection in cognitive radio using Hidden Markov Models," 2015 IEEE Advanced Information Technology, Electronic and Automation Control Conference (IAEAC), Chongqing, China, December 19-20, 2015.

[4] O'Shea, T. J., Clancy, T. C., & McGwier, R. W. (2016). Recurrent neural radio anomaly detection. arXiv preprint arXiv:1611.00301.

[5] S. Rajendran, W. Meert, V. Lenders and S. Pollin, "Un supervised Wireless Spectrum Anomaly Detection With I nterpretable Features," IEEE Transactions on Cognitive C ommunications and Networking, **5**, 3, September 2019, pp . 637-647, doi: 10.1109/TCCN.2019.2911524

[6] S. Rajendran, W. Meert, V. Lenders and S. Pollin, "SAIFE: Unsupervised Wireless Spectrum Anomaly Detection with Interpretable Features," 2018 IEEE International Symposium on Dynamic Spectrum Access Networks (DySPAN), Seoul, South Korea, October 22-25, 2018.
[7] Y. Tang, Y. Tang, M. Han, J. Xiao and R. M. Summers, "Abnormal Chest X-Ray Identification With Generative Adversarial One-Class Classifier," 2019 IEEE 16th International Symposium on Biomedical Imaging (ISBI 2019), Venice, Italy, April 8-11, 2019.
[8] Schlegl, T., Seeböck, P., Waldstein, S. M., Schmidt-Erfurth, U., & Langs, G. (2017, June). Unsupervised anomaly detection with generative adversarial networks to guide marker discovery. International conference on information processing in medical imaging (IPMI), Boone, NC, USA, June 25-30, 2017.
[9] S. Akçay, A. Atapour-Abarghouei and T. P. Breckon, "Skip-GANomaly: Skip Connected and Adversarially Trained Encoder-Decoder Anomaly Detection," 2019 International Joint Conference on Neural Networks (IJCNN), Budapest, Hungary, July 14-19, 2019.
[10] L. Deng, "The MNIST Database of Handwritten Digit Images for Machine Learning Research [Best of the Web]," IEEE Signal Processing Magazine, **29**, 6, November 2012, pp. 141-142, doi: 10.1109/MSP.2012.2211477
[11] M. Zhang, M. Gong, Y. Mao, J. Li and Y. Wu, "Unsupervised Feature Extraction in Hyperspectral Images Based on Wasserstein Generative Adversarial Network," Geoscience and Remote Sensing, **57**, 5, May 2019, pp. 2669-2688, doi: 10.1109/TGRS.2018.2876123
[12] M. Arjovsky, S. Chintala, L. Bottou, "Wasserstein generative adversarial networks", Proceedings of the 34th International Conference on Machine Learning (ICML), Sydney, Australia, August 6-11, 2017.